AIVP ADVANCES IN IMAGE AND VIDEO PROCESSING
SOCIETY FOR SCIENCE AND EDUCATION UNITED KINGDOM
VOLUME 4, ISSUE 1
ISSN 2054-7412

Evidential Segmentation Scheme of Bone Marrow Images

Mourtada Benazzouz, Ismahan Baghli, Amine BENOMAR
Med AMMAR , Youcef Benmouna, Med Amine Chikh
Genie Biomedical Laboratory, Tlemcen university
{m_benazzouz,i_baghli,mea_chikh}@mail.univ-tlemcen.dz

Abstract

The analysis of microscope images can provide useful information concerning health of patients. In this paper a new and efficient supervised method for color image segmentation is presented. The segmentation here is to extract leukocytes (white blood cells) and separate its constituents, nucleus and cytoplasm. Since red cells, leukocytes and background had different color in image of bone marrow smear, they were extracted according to their own colors. First, we train an SVM in different color spaces by a learning set. SVM with fixed parameters is used here to yield several classifications, and the basic technique consists on information fusion from different sources via evidence theory. This combination is performed by integrating uncertainties and redundancies for each one of the color spaces. From the experiments, we achieve good segmentation performances in the entire nucleus and cytoplasm segmentation. We evaluate the segmentation performance of the proposed technique by comparing its results with the cell images manually segmented by an expert.
keywords : Fusion, SVM, Evidence theory, Leukocytes, color spaces.

1 Introduction

Leukocytes or white blood cells (WBC) are cells in the blood that are involved in defending the body against infective organisms and foreign substances. When an infection is present, the production of WBCs increases. They play a significant role in the diagnosis of different diseases, and therefore, extracting information about that is valuable for hematologists. However, it is tedious and time consuming to locate, classify and count leukocytes. An automated differential counter using image analysis makes it possible to replace the work, reducing reporting time and increasing accuracy with the larger number of cell counted.

The paper presents the first step for building an automatic system of blood cell recognition, this gait consists in segmentation of blood cell images, which is a crucial step for automatic cell analysis, because the success of the final classification depends mainly on the correct image segmentation.

In an attempt to solve the problem, several approaches have been presented in the literature, most of them utilized the gray level, texture, and color [1]. Several general-purpose algorithms and techniques have been developed for image segmentation. Since there is no general solution to the image segmentation problem, these techniques often have to be combined with domain knowledge in order to effectively solve a segmentation problem for problem domain [2].

Among the common segmentation methods are edge and border detection, region growing, filtering, mathematical morphology, pixel classification and watershed clustering. A variety of semi-automatic or automatic WBC segmentation methods have been proposed. Hiremath et al. [3] presented a technique based on thresholding, morphological operators and statistical texture analysis. Chen et al. [4] used Mean Shift to extract a few significant samples as training set for pixel classification and recently [5] construct a segmentation model using simulated visual attention via learning by on-line sampling.

After a preprocessing with SMMT (Self Multiscale Morphological Toggle), Leyza et al. [6] proposed watershed transform and Level Set Methods for nucleus segmentation and granulometric analysis or morphological transformations for cytoplasm segmentation. GramSchmidt orthogonalization along with a snake algorithm have been used to segment nucleus and cytoplasm of the cells in [7]. Interesting segmentation schemes have been presented in [8] by using the Sliding Band Filter to segment blood cell and [9] by combining probability density function and a morphological operation for nucleus and cytoplasm respectively, also in [10] by using color information and means of K-means to extract nucleus.

DOI: 10.14738/aivp.41.1924
Publication Date: 29th February, 2016
URL: http://dx.doi.org/10.14738/aivp.41.1924

The use of multiple classifiers, also called classifier ensembles, is now recognized as a practical and efficient solution for solving complex pattern recognition problems [11, 12, 13, 14, 15]. The idea behind classifier ensembles is that different classifiers may potentially offer complementary information about patterns to be classified, allowing for potentially higher classification accuracy. Others fusion's studies [16, 17] shown that this technique has became more and more used to improve the quality of recognition systems in medical systems.

In this work, we propose an automatic machine-learning method (SVM) to segment blood and bone marrow cell images. Different from traditional methods of classification, we focus on a few significant samples rather than all of them. Thus samples are trained in several color spaces in order to benefit of their complementarities. A confusion of classification may remains when a same pixel belongs to different classes. Therefore fusion between pixels is taken into account via Dempster shafer's rule.

The remainder of the paper is structured as follows: in section 2 we describe microscopic images, color spaces, SVM classification and fusion's techniques. The main steps of the proposed color segmentation approach and some results are presented in section 3. Paper is concluded in section 4.

2 Methods and Materials

2.1 Microscopic Cell Images

Our images contain erythrocytes (red cells), leukocytes (white blood cells) platelets and plasma (background) (Figure 1). The red cells make up about 48% of the blood volume, and carry oxygen and carbon dioxide

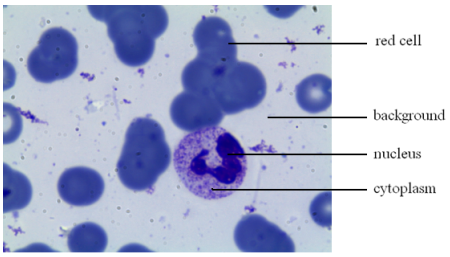

Figure 1: A bone marrow smear image

around our body. Normal blood contains 4000-10000 leukocytes/μl of blood. The Leukocytes (nucleus and cytoplasm) play a vital role in the immune system ; where they eliminate germs such as bacteria and viruses, and fight cancer cells and other toxic substances [18]. Platelets are small particles and not clinically important [19].

Our base is constructed from acquired images in hemobiology service (Tlemcen Hospital), on blades with the MGG coloration (May Grunwald Giemsa). The LEICA environment (camera and microscope) permit to obtain RGB 24-bit color pictures of 1024 per 768 with good quality format bitmap. The camera is attached to a Leica microscope with 100 objective magnification.

2.2 Color spaces

Our images come from colored blades, therefore it will be useful to exploit the color information as considered in several papers [5, 10, 7, 20].

The first step of the proposed scheme concerns the colorimetric transformation of the initial coordinates system (the RGB space). The question to investigate such transformations is: does exist a color space in which the representation of the color data is the best to optimally perform the segmentation process? Obviously, many researches have shown that no color space significantly outperforms the others [21]. Nevertheless, each color space has been designed to outperform (under its own hypothesis) the others [22].

From this remark, the segmentation process is performed through different colorimetric transformations. The results of this segmentation step are then fused in order to obtain a final segmented image. To be rather exhaustive without having to test all existing color spaces, we used five representative color spaces belonging to the four color spaces families described by [23]. Initially seven color spaces have been experimented but

our choice has focus on five color spaces: RGB (primary spaces) HSL and HSV (perceptual space), LUV (perceptually uniform spaces) and YUV (spaces of television), cause they have given best results.

The intention of the L*u*v* color space is to produce a color space that is more perceptually linear than other existing color spaces. Perceptually linear means that a change of the same amount in a color value should produce a change of about the same visual importance.

The YUV model defines a color space in terms of one luminance and two chrominance components. YUV is used in the PAL system of color encoding in analog video, which is part of television standards in much of the world. YUV models human perception of colour more closely than the standard RGB model used in computer graphics hardware, but not as closely as the HSL colour space.

The HSL colour space (Hue, Saturation, Lightness/ Luminance), is quite similar to the HSV space, also known as HSB (Hue, Saturation, Brightness). The difference is that the brightness of a pure colour is equal to the brightness of white, while the lightness of a pure colour is equal to the lightness of a medium gray. The HSL colour space is often used by artists because it is often more natural to think about a colour in terms of hue and saturation than in terms of additive or subtractive colour components [24].

As these color spaces have their own properties, it would be useful to exploit them altogether in a whole segmentation process in order to increase the quality of the results. For this reason, we opted for the use of several spaces in order to take advantage of complementarity's spaces.

2.3 Support Vector Machines

Let the training set D be $\{(x_i, l_i)\} i = 1..N$ with input x_i and $l_i = \{\pm 1\}$. SVM [25] first maps x to $y = \phi(x) \in F$. when the data is linearly separable in F, SVM constructs a hyperplane $wTz + b$ for which separation between the positive and negative examples is maximized.

It can be shown that $w = \sum_{i=1..N} \alpha_i l_i z_i$, where $\alpha = (\alpha_1, , \alpha_N)$ can be found by solving the following quadratic programming problem:

$$min \frac{1}{2} \alpha^T Q \alpha - e^T \alpha \tag{1}$$

Subject to $\alpha \geq 0$ and $\alpha^T l = 0$. Where e is the vector of all ones, $l = (l_1, ..., l_N)^T$ and Q has entries $l_i l_j z_i^T z_j = l_i l_j K(x_i, x_j)$ where $K(x_i, x_j)$ is called a Kernel. When the training set is not separable in F, the SVM algorithm introduces non-negative slack variable $\xi_i \geq 0$. The result problem becomes

$$min \frac{1}{2} \|w\|^2 + C \sum_{i}^{n} \xi_i \tag{2}$$

Subject to $l_i(w^T z + b) \geq 1 - \xi_i$. C is a regularization parameter controlling the trade off between model complexity and training error.

The x_i for which $\alpha_i \neq 0$ are defined as the support vectors, since they determine the optimal hyperplane, the hyperplane with maximal margin. Geometrically, the support vectors correspond to the closest to the optimal hyperplane. The optimal decision functions is

$$f(x) = sign(\sum_{i=1..N} \alpha_i l_i K(x_i, x) + b) \tag{3}$$

In this paper, radial basis function (RBF) is selected as the kernel of SVM, which is

$$K(x_i, x_j) = exp(-g \|x_i - x_j\|^2) \tag{4}$$

The rest parameters in training are the kernel parameter g and the regularization parameter C of SVM. The program code and more detailed discussion about C-SVM algorithm can be found at [26].

SVM being binary classifiers, $\frac{m(m-1)}{2}$ SVM classifiers are induced for a multi-class problem. A final decision is taken from the outputs of all binary SVM.

2.4 Fusion

A classifier usually designates a recognition tool that provides class membership's information for a vector received in input. This tool can be described by a function e that with a feature vector x of the object to recognize, assign to x the class Cl_i among k possible ones [27]:

$$e : x \in R^n \rightarrow K(K \in \{Cl_1, ..., Cl_k\}) \tag{5}$$

Moreover, the answers provided by the classifier can be classified in three categories [11]:

- **Class type**: $e(x) = Cl_i(i \in [1, k])$, indicates that the classifier assigned the class Cl_i to x,
- **Rank type**: $e(x) = [r_1^j, ..., r_k^j]$ where r_i^j is the assigned rank to the class i by the classifier
- **Measure type**: $e(x) = [m_1^j, ..., m_k^j]$ where m_1^j is the measure assigned to the class i by the classifier

For complex detection and classification problems involving data with large intra-class variations and noisy inputs, perfect solutions are difficult to achieve, and no single source of information can provide a satisfactory solution. As a result, combination of multiple classifiers (or multiple experts) is playing an increasing role in solving these complex pattern recognition problems, and has proven to be viable alternative to using a single classifier.

Classifier combination is mostly heuristic and is based on the idea that classifiers with different methodologies or different features can have complementary information. Thus, if these classifiers cooperate, group decisions should be able to take advantages of the strengths of the individual classifiers, overcome their weaknesses, and achieve a higher accuracy than any individual's.

Over the past few years, a variety of schemes have been proposed for combining multiple classifiers. We opted for 2 types of methods; majority vote (non trainable) and dempster shafer rule.

2.4.1 Fusion based on voting

The well known populous form of voting has gained a great usefulness in based decision fusion. In the voting based fusion the class is assigned by a classifier which has been considered and valued as a vote for that class so, we can mention in this step of study three voting versions in which the class winner has been getting an agreement with all classifiers (anonymous voting) predicted generally by one more then half the classifier's number (simple majority), or that receives the highest number of vote whether or not the sum of those vote attains 50 % (pluarlity voting or just majority voting). the well known popular is the vote majority in which the voted class taking into consideration most of classifiers will be regarded and valued or estimated as winner and the input is assigned to that class [28].

2.4.2 Fusion based on evidence theory

Major concepts of this theory are briefly reviewed in the following.
Suppose there is a finite set of mutually exclusive and exhaustive hypotheses $\Omega = \{w_1, ..., w_n\}$ called the frame of discernment. A basic belief assignment (BBA) or mass function is a function $m : 2^\Omega \rightarrow [0, 1]$, in which 2^Ω is the number of all possible subset of Ω and it satisfies two conditions as mentioned below:

$$\begin{cases} m(\phi) = 0 \\ \sum_{A \subseteq \Omega} m(A) = 1 \end{cases} \tag{6}$$

If A is considered as a subset of $\Omega (A \subseteq \Omega)$, $m(A)$ indicates the degree of belief that is assigned to the exact set A and not to any subsets of A. There are also the following two definitions in the theory of evidence that are derived from mass function:

$$\begin{cases} Bel(A) = \sum_{B \subseteq \Omega} m(B) \\ Pl(A) = \sum_{A \cap B \neq \phi} m(B) \end{cases} \tag{7}$$

Apart from strength of the evidence theory in specifying a degree of uncertainty, it can also combine different evidences to increase certainty value which results in more accurate decisions.
The method of combining different evidences using Dempsters rule is also called orthogonal sum in which two independent information sources (m_1 and m_2) are fused to create a new belief function as shown below:

$$m(C) = \frac{\sum_{A \cap B = C} m_1(A) \times m_2(B)}{1 - \sum_{A \cap B = \phi} m_1(A) \times m_2(B)} \tag{8}$$

Where the denominator can be interpreted as a conflict criterion between independent evidences to be combined [29].

3 Experimentation and results

Twenty seven microscopic images were used to evaluate the proposed segmentation algorithm. Each one containing cells and all segmented manually by a medical expert in cytopathology to further assess the recognition quality (Figure 2).

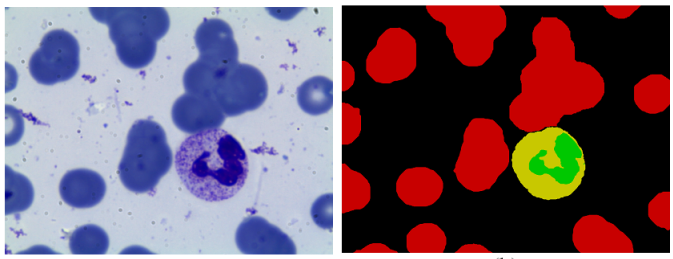

(a) (b)

Figure 2: Original image (a), ground truth image (b)

3.1 Training set

After image acquisition, we notice an intraclass variability, which induce us to choose the most representative samples. We took significant samples from 9 images to construct a learning set and the classification has been applied on the rest. Different regions were selected from each class (Figure 3); they will form the reference training set, since our blades undergo the same coloration MGG. We use this set to construct an SVM classifier for each colour space; the inputs of each SVM are the values of the pixel in its colour space.

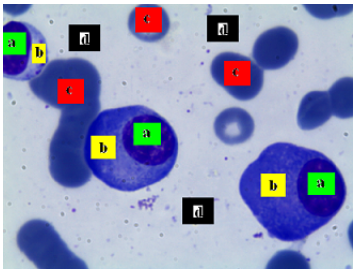

Figure 3: (a)nucleus region (b) cytoplasm region (c)erythrocyte region (d)background region

The SVM parameters c and g were optimized after using multiple-fold cross validation. that is often an off-line task in practice, which leads to the following parameters c=512 and g=0.0001.

3.2 Results

In table 1, we present in order of merit the results of single pixel classifications obtained with all colour space to further justify the importance of the combination step.

	Nucleus	Cytoplasm	Red Cell	Background
HSL	77.17%	31.63%	87.82%	98.95%
HSV	78.01%	38.12%	92.20%	98.76%
RGB	92.23%	40.45%	97.43%	98.47%
LUV	93.53%	29.18%	97.46%	98.11%
YUV	93.35%	41.85%	97.52%	92.52%

Table 1: Obtained accuracy for colour spaces

The first observation is that the class cytoplasm present the lower scores, and this is due to the variability of its constituent pixels. which create confusion with red blood cells. Moreover, Figure 4 shows that the separation between red blood cell and cytoplasm is not obvious; the SVM tries to find the separation in space of higher dimension.

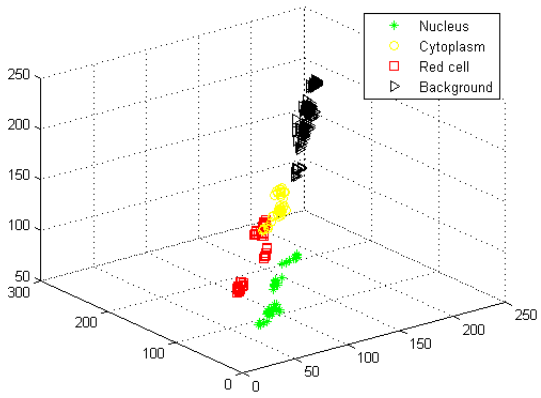

Figure 4: Classes projection

A pixel is called conflicting if it is classified differently in different spaces. In order to generate the final segmentation map, the intersection of the obtained maps within each one of the trial colour spaces is achieved. Only conflicting pixels are processed using the theory of evidence. The introduction of the fusion begins with untrained method (majority vote), then different models of the theory of evidence are presented in Table 2.

We chose two different mass functions, one is directly extracted from the confusion matrix named mass1 and the other along the following Denoeux's principle named mass2 [30, 31]:

$$\begin{cases} m(w_i) = \alpha \exp(-\gamma_l d^2) \\ m(\Omega) = 1 - m(w_l) \end{cases} \tag{9}$$

Where $0 < \alpha < 1$ is a constant computed from the obtained a posteriori probabilities provided by the SVM output for the class w_l within the trial colour spaces.
The γ parameter is used to modify the effect of distance in the calculation of the mass and d is the Euclidean distance between the current pixel and the means characteristic of the class. It was proposed [32] to set $\alpha = 0.95$ and $\gamma = 0.05$.

The evidence theory offers various modeling assumptions, we opted for two choices: the first hypothesis (h1) considering only the output class and its complement in the space of discernment, we have noted by $h1(i)$ and $h1(j_1, j_2, j_3)$. And the second hypothesis taking each output with the others one by one: $h2(i)$, $h2(i, j_1)$, $h2(i, j_2)$ and $h2(i, j_3)$; where i represent the output of the classifier and j_1, j_2, j_3 the others outputs different from i.
The first hypothesis was tested using the two mass functions and the second only with mass1 function.

The combination with previous models is realized by two orthogonal sum rules: the associativity (rule1) between the mass functions [30, 31], or grouping of mass functions according to their outputs (rule2) [32].

From the previous stated, we combine two mass functions (mass1 and mass2) with the two sum rules (rule1 and rule2) according to the two hypotheses (h1 and h2). This has resulted in six fusion experimentation in addition to the majority vote, and the results of accuracy and classification rate are presented in Table 2 and 3.

Figure 5 shows the process of segmentation applying the proposed method under the hypothesis above.

3.3 Discussion

Our choice for the SVM classifier is justified by high classification rate and fast pixel classification process. The experimentation has demonstrated a proposed scheme for segmenting blood cells using integration of uncertainties and redundancies for each colour space, contrary to majority vote which gives sporadic results; not based on any learning theory.

	Nucleus	Cytoplasm	Red Cell	Background
Majority vote	86.26%	41.93%	96.89%	98.53%
Theory1(H1,mass1,rule1)	91.76%	44.12%	96.98%	98.43%
Theory2(H1,mass1,rule2)	80.99%	40.39%	96.48%	98.49%
Theory3(H1,mass2,rule1)	74.43%	40.63%	86.74%	98.97%
Theory4(H1,mass2,rule2)	74.43%	40.63%	86.74%	98.97%
Theory5(H2,mass1,rule1)	92.59%	39.93%	97.19%	98.52%
Theory6(H2,mass1,rule2)	96.62%	48.81%	93.67%	98.08%

Table 2: Obtained accuracy for Fusion

	Nucleus	Cytoplasm	Red Cell	Background
Theory1(H1,mass1,rule1)	94.50%	88.72%	75.72%	96.32%
Theory2(H1,mass1,rule2)	94.46%	89.63%	65.62%	96.60%
Theory3(H1,mass2,rule1)	87.30%	80.41%	63.86%	87.47%
Theory4(H1,mass2,rule2)	87.30%	80.41%	63.86%	87.47%
Theory5(H2,mass1,rule1)	93.25%	89.51%	75.32%	95.11%
Theory6(H2,mass1,rule2)	84.71%	82.25%	78.48%	97.51%

Table 3: Obtained classification rate for Fusion

Nucleus segmentation is highly satisfactory even without requiring fusion. However, statistical analysis on the conflicting pixels revealed that the most of them belong to the cytoplasm and red cell classes, hence the necessity of combination(fig6 and table 4).

	Nucleus	Cytoplasm	Red Cell	Background
Conflicting pixels	85076	184119	754416	1719458
Corrected pixels	64898	127280	592426	1668646

Table 4: Conflicting pixels

Based on the numerical results, and especially the visual quality of the segmentation, we distinguish two models (theory1 and theory6) with the function mass1 that gave better accuracy. Also considering the same hypothesis, the sum rules affect the outputs (theory1/theory2 and theory5/theory6). Note that lower scores were recorded for models 3 and 4 who had the same behavior. However, the recognition rates show us that theory1 is best for correcting conflicting pixels. From the images tested, we observed that 89% of the conflicting pixels have been corrected.

The original images contain red blood cells with a clear area in the center, this led the SVM detect red cell's center as a background. But this misclassification does not affect the result since this kind of cells does not contribute to the diagnostic. It can be corrected by filling operation. A post-processing is needed to improve the quality of the segmentation; achieved by elimination of artifacts, and also by removing the small red areas in the cytoplasm region.

The major errors were caused by the following reasons. First, misclassification occurs mainly between closely related classes (red cells and some cytoplasm regions), no distinction is made between them. Second, when cytoplasmic granules are as dark as a nucleus or a cytoplasm as bright as a background, they are classified as a nucleus and a background, respectively. Our post-processing has tried to overcome these shortcomings cited above by eliminating small regions detected as background inside the cytoplasm and also by eliminating small regions detected as nucleus inside the cytoplasm.

Even the diagnostic of experts, is based essentially on leukocyte characteristics. Indeed, our segmentation focus on this type of cell which includes nucleus and cytoplasm (Region Of Interest). After post-processing we obtained the following accuracy and classification rate(table 5):

The results show that the proposed method is able to yield 96.42% accuracy for nucleus segmentation and 50.77% for cytoplasm segmentation. (Figure 7)

We found useful to add some visual results (Figure 8) from several regions of interest to justify the

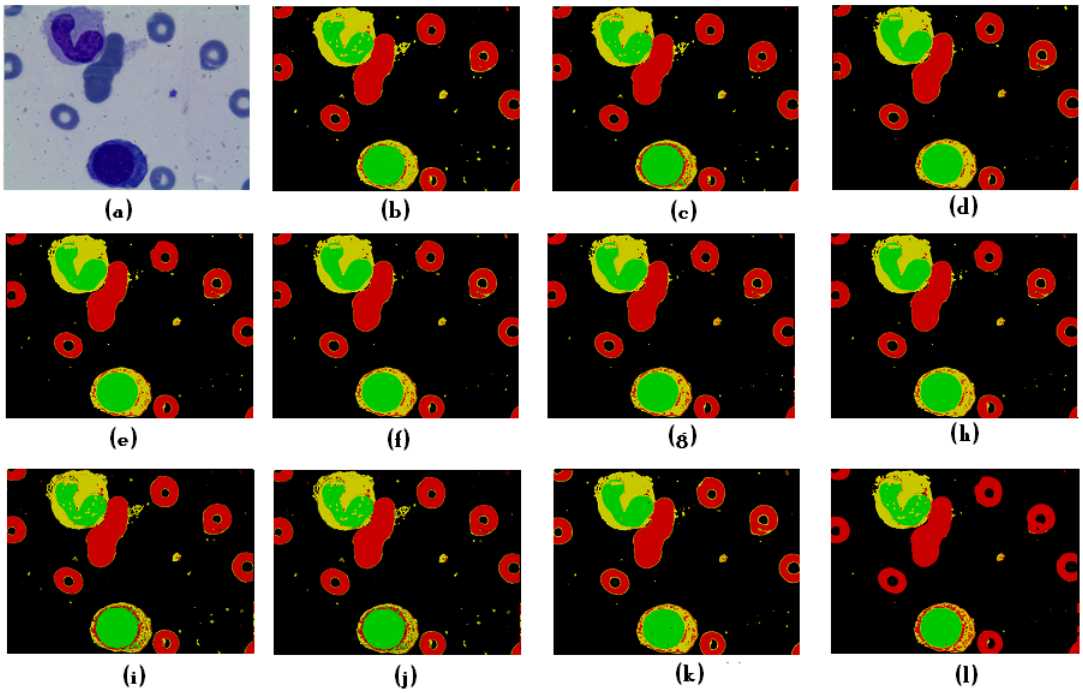

Figure 5: (a) Original image (b) HSL result (c) HSV result (d) RGB result (e) LUV result (f) YUV result (g) Theory1 result (h) Theory2 result (i) Theory3 result (j) Theory4 result (k) Theory5 result (l) Theory6 result

Theory1	**Nucleus**	**Cytoplasm**
Accuracy	96.42%	50.77%
Classification rate	93.53%	90.04%

Table 5: Obtained accuracy after post-processing

unconvincing accuracy of the cytoplasm which are mostly due to misclassification in other regions such as artifacts and platelets.

Our images are noisy (not pretreated images), and often contain overlapping and condensed cells. In contrast to other methods based on morphology or thresholding, our strategy can achieve higher accuracy of segmentation especially in complex scenes where watershed, region growing and others have struggling to segment. In our recent scientific works, we propose a segmentation scheme using pixel classification based on the fusion of information. The adopted model is guided by the two strategies offered by information fusion, i.e. classifying separately the data from different sources then merging decisions(what was done in the present paper), or combining these data to classify them(made in a previous publication [33]).

Automatic recognition of white blood cells in light microscopic images usually consists of major steps, including: image segmentation, feature extraction and classification. Here, our aim is to accurately segment the nucleus and cytoplasm components of blood smear images, to further extract attribute for automated differential counting. According to medical experts, different characteristics of nucleus and cytoplasm are important features for discrimination of certain leukocyte types. We plan to realize an approach that require one sub-image for each WBC, and from this sub-image several types of features can be extracted; texture features, shape features in addition to color features.

4 Conclusion

In this paper, we propose a fusion scheme of colour image segmentation. Our strategy is applicable to noisy images. Trained SVMs are performed to define separation between classes, followed by segmentation in

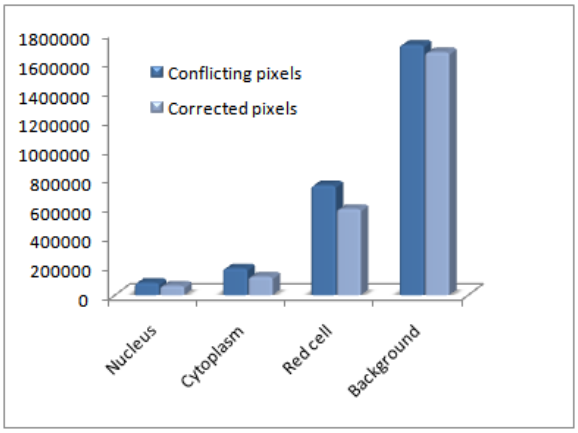

Figure 6: Correction rate

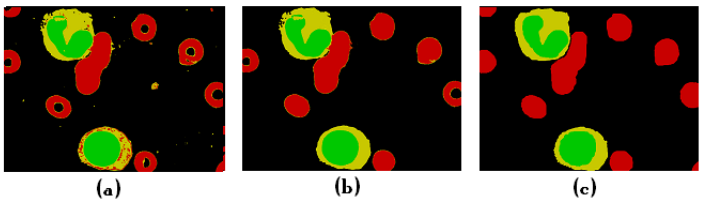

Figure 7: (a) Fusion result (b) Post-processing result (c) Ground truth

different colour spaces and a final decision is taken by dempster shafer's rule.

Our framework has achieved a considerable improvement on the segmentation; among the conflicting pixels, most of them have been well classified i.e an improvement of 89% by the use of the concepts of evidence theory.

Future work are envisaged by adding texture attributes to color spaces and proceed to the characterization stage in order to recognize cell's type.

5 Acknowledgments

Our team have completed the acquisition of microscopic images and the annotation (labeling) of the different regions (classes). This base did not exist without the contribution of Mrs. N. Benmansour (Hemobiology service, Tlemcen Hospital) who opened her service and gave us access to the LEICA microscope and patients slides. We wish to thank her and express our gratitude.

References

[1] K.Y. Lin, J.H. Wu, and L.H. Xu. A survey on color image segmentation techniques. *Journal of Image and Graphics*, 10(1):1–9, 2005.

[2] Pascal Bamford. *Empirical Comparison of Cell Segmentation Algorithms Using an Annotated Dataset.* PhD thesis, University of Queensland, Brisbane, Australia, 2003.

[3] Hiremath P.S., Bannigidad Parashuram, and Geeta Sai. Automated identification and classification of white blood cells (leukocytes) in digital microscopic. *IJCA Special Issue on 'Recent Trends in Image Processing and Pattern Recognition'*, pages 59–63, 2010.

[4] Pan Chen, Lu Huijuan, and Cao Feilong. Segmentation of blood and bone marrow cell images via learning by sampling. *ICIC 2009*, pages 336–345, 2009.

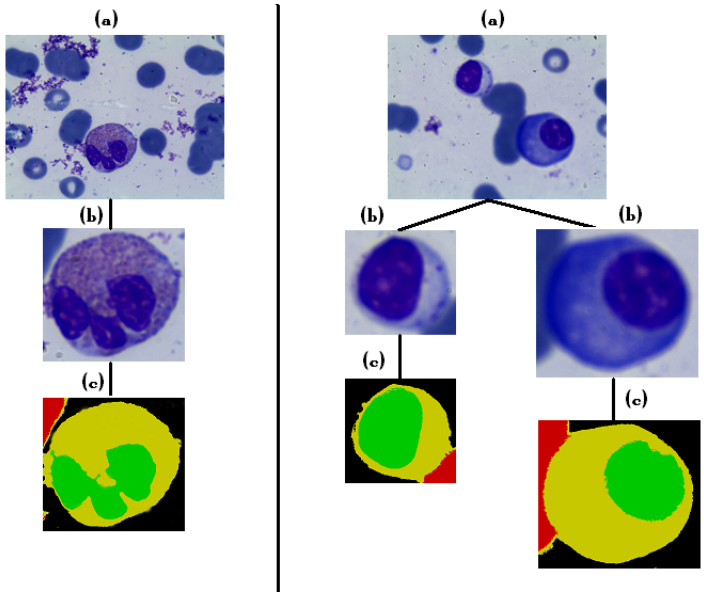

Figure 8: (a) Original image (b)Region Of Interest (c)Segmented region

[5] Chen Pan, Dong Sun Park, Sook Yoon, and Ju Cheng Yang. Leukocyte image segmentation using simulated visual attention. *Expert Systems with Applications*, 39:74797494, 2012.

[6] Leyza Baldo Dorinin, Rodrigo Minetto, and Neucimar Jeronimo Leite. Semi-automatic white blood cell segmentation based on multiscale analysis. *IEEE Trans Inf Technol Biomed*, In press, 2012.

[7] Seyed Hamid Rezatofighi and Hamid Soltanian-Zadeh. Automatic recognition of five types of white blood cells in peripheral blood. *Computerized Medical Imaging and Graphics*, 35:333343, 2011.

[8] Quelhas P., Marcuzzo M., Mendonca A.M., and Campilho A. Cell nuclei and cytoplasm joint segmentation using the sliding band filter. *IEEE Transactions on Medical Imaging,*, 29:14631473, 2010.

[9] Ko BC, Gim JW, and Nam JY. Automatic white blood cell segmentation using stepwise merging rules and gradient vector flow snake. *MICRON*, 42:695–705, 2011.

[10] Ramin Soltanzadeh, Hossein Rabbani, and Ardeshir Talebi. Extraction of nucleolus candidate zone in white blood cells of peripheral blood smear images using curvelet transform. *Computational and Mathematical Methods in Medicine*, In press, 2012.

[11] Roli F. and Giacinto G. Design of multiple classifier systems. *Hybrid methods in pattern recognition*, 2002.

[12] Goumas Stefanos K., Dimou Ioannis N., and Zervakis Michalis E. Combination of multiple classifiers for post-placement quality inspection of components: A comparative study. *Information Fusion*, 11:149–162, 2010.

[13] Mahdi Tabassian, Reza Ghaderi, and Reza Ebrahimpour. Knitted fabric defect classification for uncertain labels based on dempstershafer theory of evidence. *Expert Systems with Applications*, 38:5259–5267, 2011.

[14] Rottensteiner Franz, Trinder John, Clode Simon, and Kubik Kurt. Using the dempstershafer method for the fusion of lidar data and multi-spectral images for building detection. *Information Fusion*, 6:283–300, 2005.

[15] Hicham Laanaya, Arnaud Martin, Driss Aboutajdine, and Ali Khenchaf. Support vector regression of membership functions and belief functions application for pattern recognition. *Information Fusion*, 11:338–350, 2010.

[16] A.-S. Capelle, O. Colot, and C. Fernandez-Maloigne. Evidential segmentation scheme of multi-echo mr images for the detection of brain tumors using neighborhood information. *Information Fusion*, 5:203–216, 2004.

[17] Zhang Nan, Ruan Su, Lebonvallet Stephane, Liao Qingmin, and Zhu Yuemin. Kernel feature selection to fuse multi-spectral mri images for brain tumor segmentation. *Computer Vision and Image Understanding*, 115:256–269, 2011.

[18] W. Lin, J. Xiao, and E. Micheli-Tzanakou. A computational intelligence system for cell classification. *IEEE international conference on information technology applications to biomedecine*, May 1998.

[19] Adollah R., Mashor M.Y., Mohd Nasir N.F., Rosline H., Mahsin H., and Adilah H. Blood cell image segmentation: A review. *Biomed 2008, Proceedings*, 21:141–144, 2008.

[20] K. Jiang, Q. Liao, and Y. Xiong. A novel white blood cell segmentation scheme based on feature space clustering. *Soft Computing*, 10:12–19, 2006.

[21] Meas-Yedid V., Glory E., morelon E., Pinset Ch., Stamon G., , and Olivo-Marin J-C. Automatic color space selection for biological image segmentation. *IAPR 17th International Conference on Pattern Recognition*, 3:514–517, August 2004.

[22] Cyril Meurie, Olivier Lezoray, Louahdi Khoudour, and Abderrahim Elmoataz. Morphological hierarchical segmentation and color spaces. *International Journal of Imaging Systems and Technologies*, 20:167178, 2010.

[23] N. Vandenbroucke. *Segmentation d'images couleur par classification de pixels dans des espaces d'attributs colorimtriques adapts. Application l'analyse d'image de football.* PhD thesis, University of Lille 1, France, 2000.

[24] Andreas Koschan and Mongi Abidi. *Digital color image processing.* John Wiley and Sons, Inc, 2008.

[25] V. Vapnik. *Statistical Learning Theory.* John Wiley and Sons, Chichester, 1998.

[26] Chih-Chung Chang and Chih-Jen Lin. flibsvmg: A library for support vector machines. *ACM Transactions on Intelligent Systems and Technology*, 27(2,3):1–27, 2011. Software available at http://www.csie.ntu.edu.tw/cjlin/libsvm.

[27] H. Zouari, L. Heutte, Y. Lecourier, and A. Alimi. An overview of classifier combination methods in pattern recognition. *RFIA'2002*, 2:449–508, 2002.

[28] K. Ghosh, Y. Seng Ng, and R. Srinivasan. Evaluation of decision fusion strategies for effective collaboration among heterogeneous fault diagnostic methods. *Computers and Chemical Engineering Vol*, 35:342–355, February 2011.

[29] M. Tabassian, R. Ghaderi, and R. Ebrahimpour. Knitted fabric defect classification for uncertain labels based on dempster-shafer theory of evidence. *Expert Systems with Applications*, 38:5259–5267, May 2011.

[30] T. Denoeux. A k-nearest neighbor classification rule based on dempster-shafer theory. *IEEE Transactions on Systems, Man and Cybernetics*, 25(5):804–813, 1995.

[31] L. M. Zouhal and T. Denoeux. An evidence-theoritic k-nn rule with parameter optimization. *IEEE Transactions on Systems, Man and Cybernetics*, 28:263–271, 1998.

[32] Salim Chitroub. combinaison de classifieurs : une approche pour l'amlioration de la classification d'images multisources/multidates de tldtection. *Tldection*, 4(3):289–301, 2004.

[33] Mourtada Benazzouz, Ismahan Baghli, and Med Amine Chikh. Microscopic image segmentation based on pixel classification and dimensionality reduction. *International Journal of Imaging Systems and Technology*, 23(1):22–28, 2013.

